

Effect of the attachment of ferromagnetic contacts on the conductivity and giant magnetoresistance of graphene nanoribbons

S. Krompiewski

Institute of Molecular Physics, Polish Academy of Sciences, ul. M. Smoluchowskiego 17, 60179 Poznań, Poland

Abstract.

Carbon-based nanostructures and graphene, in particular, evoke a lot of interest as new promising materials for nanoelectronics and spintronics. One of the most important issue in this context is the impact of external electrodes on electronic properties of graphene nanoribbons (GNR). The present theoretical method is based on the tight-binding model and a modified recursive procedure for Green's functions. The results show that within the ballistic transport regime, the so called end-contacted geometry (of minimal GNR/electrode interface area), is usually more advantageous for practical applications than its side-contacted counterpart (with a larger coverage area), as far as the electrical conductivity is concerned. As regards the giant magnetoresistance coefficient, however, the situation is exactly opposite, since spin-splitting effects are more pronounced in the lower conductive side-contacted setups.

PACS numbers: 81.05.ue, 75.47.De, 73.23.Ad

1. Introduction

Different contact configurations affect the conductivity, and thereby also giant magnetoresistance (GMR) in the case of ferromagnetic electrodes. Here we study two most common geometries, *viz.* the end-contacted (EC) geometry and the side-contacted (SC) one. In the former the interface area is minimal, whereas in the latter a finite coverage area exists. Theoretically, it is easier to work with EC setups rather than, experimentally more relevant, SC ones. The former approach might be justified when a nanostructure/electrode coupling is strong (good transparency of interfaces, weak chemical bonding). There are experimental evidences supporting this view. In particular, Mann et al. [1] were able to control a length of CNT (carbon nanotube) under a metal contact and showed that ballistic transport in Pd/CNT occurred basically at the edges. Moreover, in similar systems, no observable difference in I-V characteristics between side-contacts and end-contacts was found [2]. In general, however the contact configuration does matter; as shown in [3] for Pd and Ti contacted carbon nanostructures. Likewise, *ab initio* studies in [4] show that in the case of ultra-small graphene nanoribbons, the EC configuration outperforms the SC one, since a large interface area may worsen the contact conductance.

As concerns ferromagnetic electrodes, it has been shown that in order for a transition metal/graphene junction to have good spin transport properties it is necessary that no strong chemical bonds (engaging graphene's π electrons) are formed [5, 6]. Although in the case of typical ferromagnetic electrodes this requirement is hardly fulfilled [7], adsorption of graphene (e.g. on Ni or Co) can be effectively weakened by introducing a protective interfacial monolayer of Cu [5]. Noteworthy, high-performance ferromagnetic-metal/graphitic-nanostructure contacts have already been reported for $\text{Ni}_{1-x}\text{Pd}_x$ with $x \sim 0.3 \div 0.5$ (see [8] and references therein).

Although the EC geometry is much more frequently used by theoreticians just for reasons of computational convenience ([9]-[14]), the issue of side-contacted nanostructures has already also been raised, see [3, 4, 13, 15] (paramagnetic electrodes) and [6, 7, 16] (ferromagnetic electrodes). In this study we treat both the geometries on the equal footing, and show how the corresponding transport characteristics (conductivity, shot noise Fano factor and giant magnetoresistance) compare with each other.

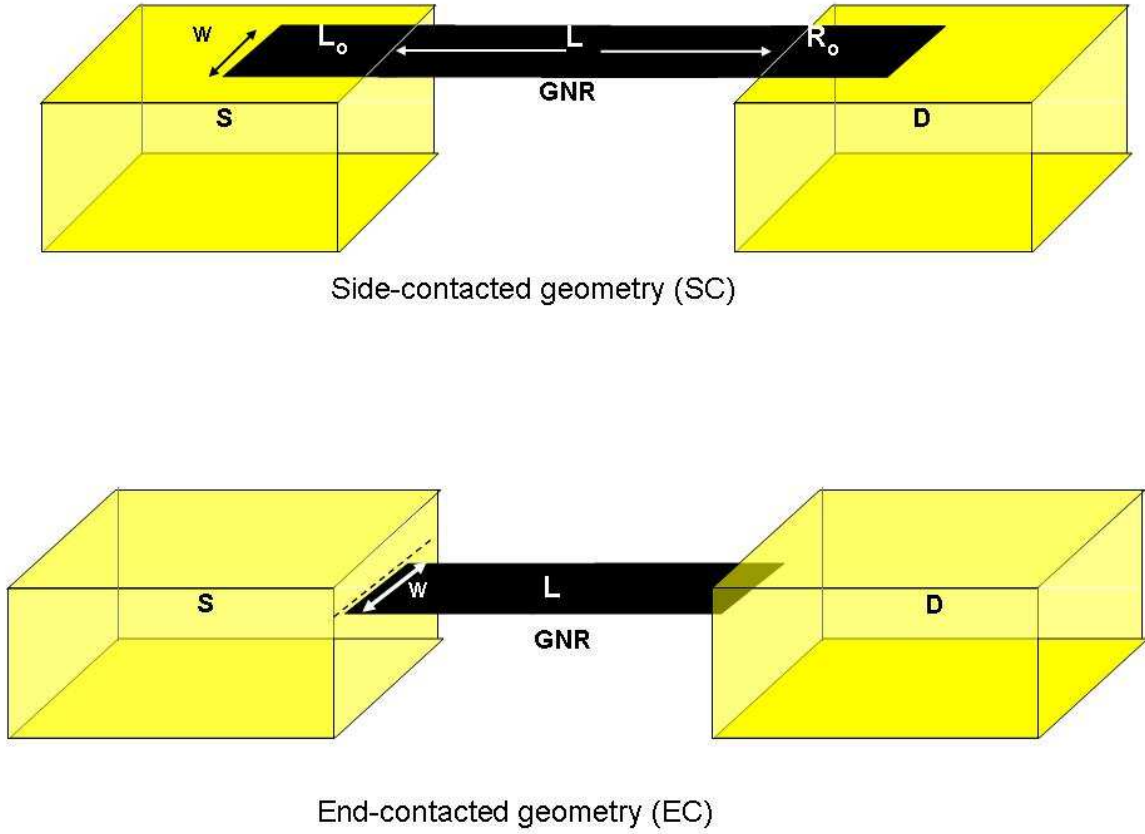


Figure 1. (Color online) Schematics of the side-contacted and end-contacted setups. S and D denote the source and drain electrodes. The GNR is drawn in black, and W , L , L_0 and R_0 stand for its width, suspended length and electrode-supported lengths, respectively.

2. Method and Modelling

We study graphene nanoribbons with infinite 3-dimensional metallic electrodes. Details on modelling and the computation method may be found in [14, 17]. However, for completeness, the most important definitions are listed below.

$$g_{ss',s''} = (L/W) \frac{e^2}{h} \text{Tr}(T_{ss',s''}),$$

$$F_{ss'} = 1 - \frac{\text{Tr}(T_{ss',\uparrow}^2 + T_{ss',\downarrow}^2)}{\text{Tr}(T_{ss',\uparrow} + T_{ss',\downarrow})},$$

$$GMR = 100 \left(1 - \frac{g_{\downarrow,\uparrow} + g_{\uparrow,\downarrow}}{g_{\uparrow,\uparrow} + g_{\uparrow,\downarrow}} \right).$$

Here g is the conductivity of the GNR, having width W and length L , for the parallel or antiparallel alignments of electrode magnetizations ($ss' = \uparrow\uparrow, \uparrow\downarrow$, respectively). $T_{ss',s''}$, in turn, stands for the transmission matrix of s'' -spin electrons in the ss' configuration. Finally, GMR is a giant magnetoresistance coefficient.

The modified recursion procedure for SC setups is carried out stepwise. The vertical contribution to the transmission matrix is related with the self-energy $\Sigma_S^I = T_{I0,IS} g_S^I T_{IS,I0}$, where I=L (R) is the left (right) electrode index, IS (I0) enumerates electrode (graphene) interface atoms and g_S is the surface Green's function matrix of the electrodes. The starting local Green's functions are defined as $g_0^L = (E - D_{L0} - \Sigma_S^L)^{-1}$, $g_{N+1}^R = (E - D_{R0} - \Sigma_S^R)^{-1}$, where L0 (R0) are the electrode-supported parts of the GNR (with the matrices of hopping integrals D), whose suspended part extends from the periodicity unit number 1 up to N. Figure 1 schematically shows the systems under consideration, and defines the end-contacted and side-contacted geometries.

The calculations have been carried out using a single-band (π orbital) tight-binding Hamiltonian, with the GNRs strongly coupled to infinite ferromagnetic external electrodes (assumed to be 50% spin-polarized), and the adopted approach is based on the Landauer type formalism. As mentioned in Sec.1 quasi-ballistic transport in carbon nanostructures has been reported in numerous papers (e.g. [15],[18]-[21]). Here we ensure a good transparency of the GNR/contact interface by defining the hopping

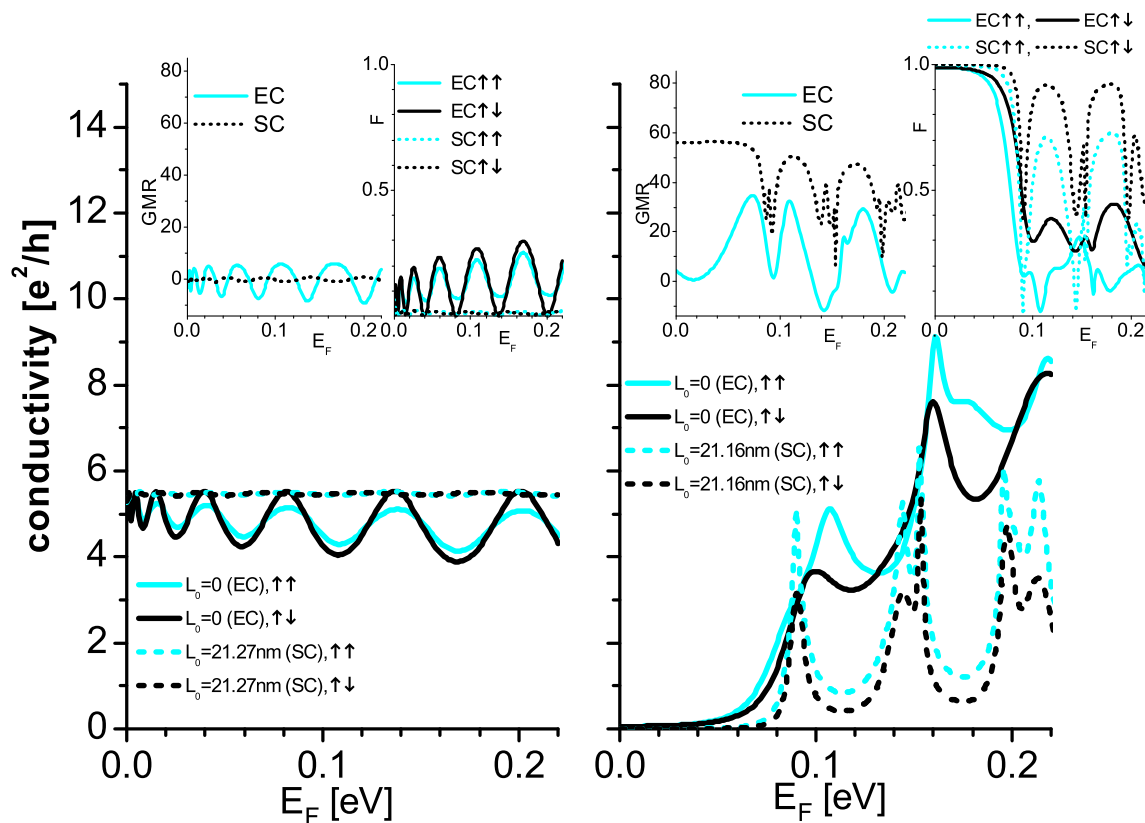


Figure 2. (Color online) The metallic zigzag GNRs and the semiconducting armchair GNRs of comparable sizes ($W \sim 8\text{nm}$, $L \sim 22\text{nm}$, and $A \sim 1/3$), with the indicated electrode-supported lengths L_0 : conductivities (main panels), GMR coefficients (left Insets), and shot noise Fano factors (right Insets). The parallel (antiparallel) electrode alignment is marked with $\uparrow\uparrow$ ($\uparrow\downarrow$).

integral across the interface as a geometrical mean of the respective hopping integrals of the GNR and the electrode (*cf.* [9, 14]).

3. Discussion of the Results

In the SC case the transport properties depend on the interface area. For small area interfaces the results are similar to those corresponding to the EC geometry, otherwise the results converge with the increasing area. In what follows, the SC results, which will be presented, correspond to the GNR/electrode coverages large enough to guarantee the convergence. The representative results are presented in Figs. 2-4, as a function of the GNR Fermi energy which is experimentally controllable by gate voltage. The aim is to elucidate the role of the interface character (EC *vs.* SC), the aspect ratio ($A=W/L$) and the current flow direction (zigzag *vs.* armchair) on spin-dependent transport in 2-terminal setups with ferromagnetic contacts. The convention adopted here is the following: solid lines apply to the EC geometry, dashed lines - to the SC geometry, whereas the cyan (brighter) curves and the black ones correspond to the parallel and antiparallel alignments of the ferromagnetic electrodes, respectively. The figures 2-3 correspond to the metallic zigzag GNRs and the semiconducting armchair GNRs of

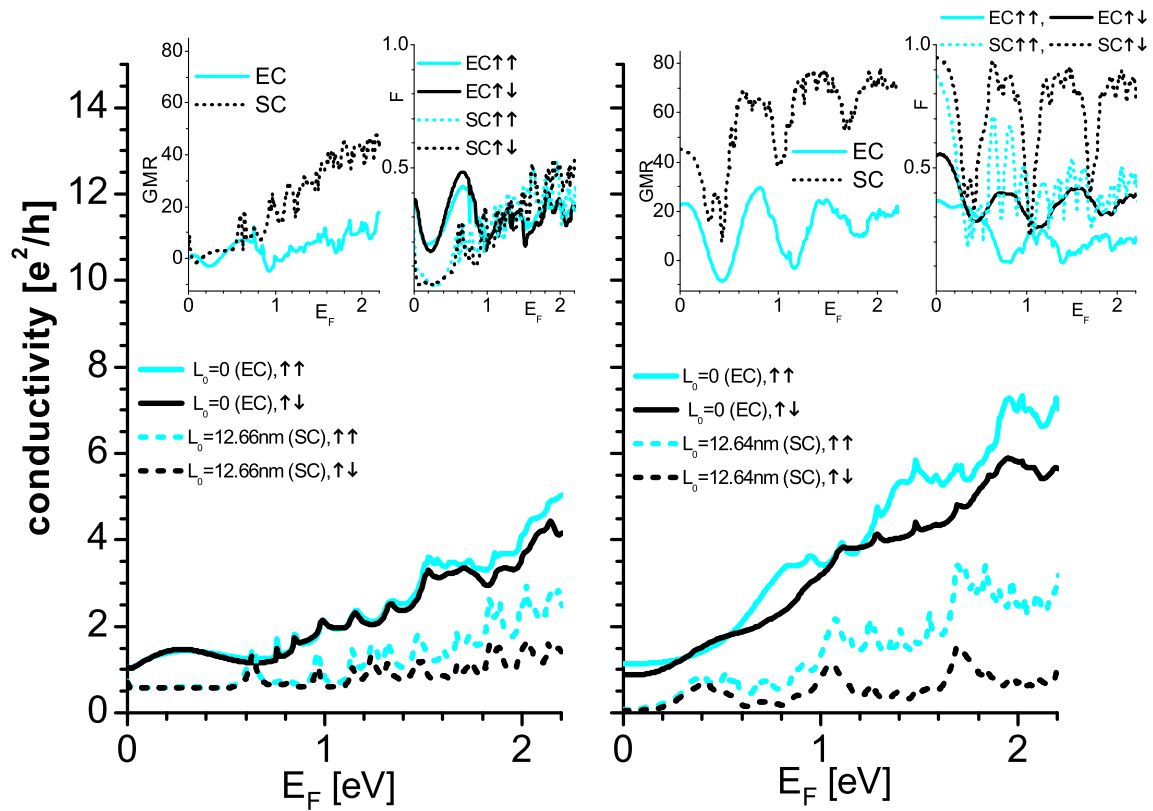


Figure 3. (Color online) As Fig. 2 but for the short systems with the aspect ratio $A \sim 3.5$.

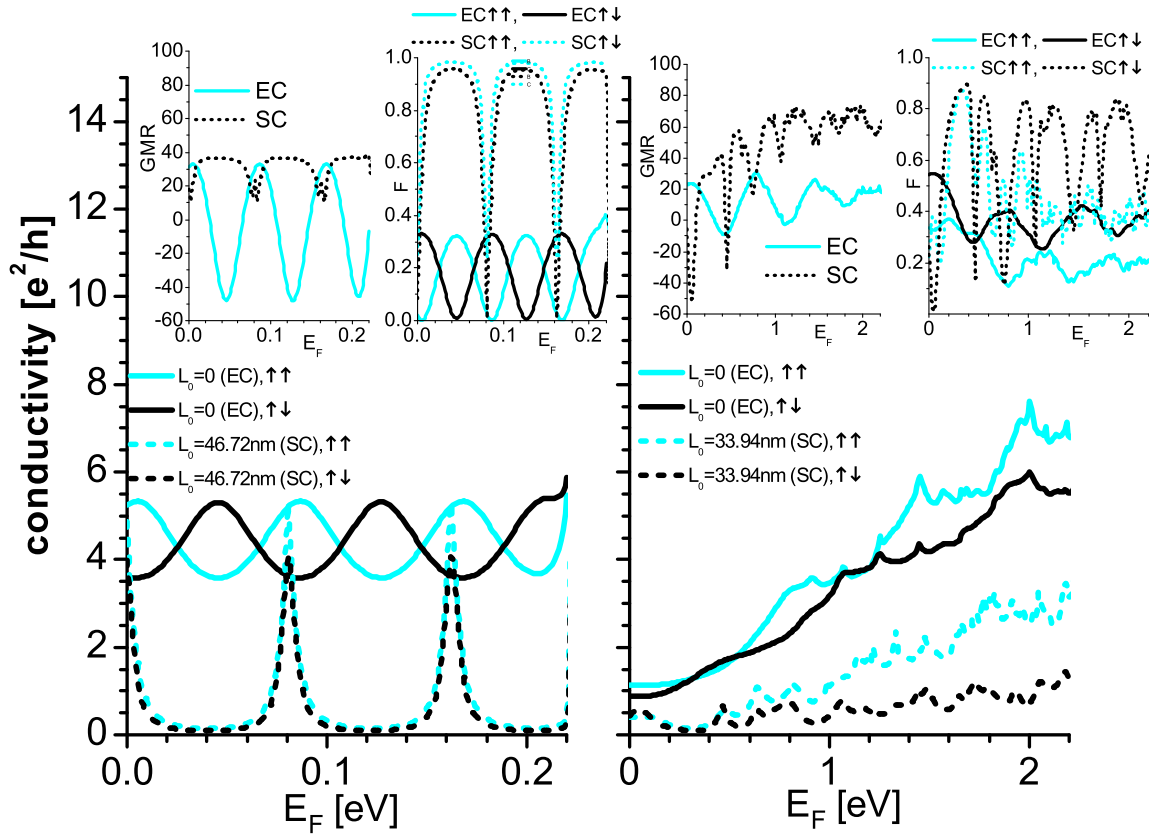


Figure 4. (Color online) Spin-dependent conductivities, GMRs and Fano factors for metallic armchair GNRs in the end- and side- contacted geometry.

comparable sizes. In shorthand notation the systems in question are: zz19-90 and ac35-52 (Fig. 2), and zz19-10 and ac35-6 (Fig. 3), where the first number denotes the GNR's width and the second one (after the hyphen) refers to the suspended length, all these numbers are expressed in periodicity units appropriate for the given direction. Remarkably, for a sufficiently long coverage length (L_0) the long zigzag GNR reveals a saturation effect as concerns the spin-dependent conductivity (at conductance = A -conductivity $\sim 2e^2/h$), resulting in gradually vanishing of both GMR and F . These features may be understood, as due to development of a low-energy perfectly conducting channel with no backscattering counterpart (*cf.* a paramagnetic electrode case of [17]). Interestingly the results for the EC and SC configuration do not differ much in the zigzag case; in other cases the respective differences are larger, unless the electrode/GNR overlap is substantially smaller than the indicated SC values of L_0 in the figures. It has been recently shown by *ab initio* calculations that Ni/GNR/Ni setups, with very small overlap lengths (up to 8\AA), have almost identical contact resistivities which moreover are independent of the current orientation [16]. It should be stressed in this context that the present phase-coherent transport theory overestimates interference processes, which in reality may be suppressed by diffusive and dephasing mechanisms. Anyway, within this

approach the conductivity does depend on the current propagation direction unlike [16] but in accord with [22, 23]. Most probably this discrepancy comes from different aspect ratios of the studied systems. Noteworthy, the present theory correctly reproduces the so-called universal minimum conductivity value predicted theoretically [24] and confirmed experimentally [20, 25], since the low-energy conductivities corresponding to the high aspect ratio EC systems are close to $4e^2/(h\pi)$ (see Figs. 3-4).

Figure 4 shows the results for nominally metallic armchair GNR ac34-52 and ac34-6 of different length. The former (longer) reveals pronounced Fabry-Pérot oscillations, resulting from the linear energy spectrum in this case. Both the systems behave similarly to the other armchair systems discussed so far, in particular the conductivities corresponding to the ES geometry are clearly higher than those referring to the SC geometry. At the same time, the EC Fano factors are, on average, lower than the SC ones. So, the EC geometry seems to be optimal for nanoelectronic applications. However the accompanying spin effects - spin splitting of the conductivities and the GMR - are most often the strongest in the side contacted systems.

The difference in conductances between the EC and SC configurations provides information about a contact resistance. If both the conductances are roughly equal to each other than the contact is characterized just by the channel width, otherwise the areal component comes into play [7]. It turns out that the contact resistances may be vanishingly small, especially at gate-controllable resonances (see Figs 2 and 4). Incidentally, very small contact resistances have been experimentally found, as well, in nearly ballistic graphene/metal junctions [15]. In the case of more complicated electrodes than those studied here, extra contributions to the contact resistance can be important (e.g. spreading resistance [26, 27]). It is so, when an STM (STS) tip is used as an electrode and/or there is a constriction in the system. In the context of spintronics related studies of graphene, it should be also mentioned that apart from the GMR also the spin-torque-transfer (STT) problem is crucial for magnetic memory applications. These two akin phenomena are due to a long spin-relaxation length in carbon nanostructures and, in principle, the present method has a potential to describe the STT, too; obviously when one of the electrodes is a non-massive free layer (see [22, 23, 28] for SST in EC-type setups).

4. Summary

In conclusion, the present quasi-ballistic theory shows that, spin-dependent transport through GNRs, depends on their aspect ratio, the GNR/electrode interface, and the current direction. It turns out that the conductivity of the semiconducting GNRs, as well as that of the nominally metallic armchair GNRs, is clearly higher in the EC geometry than in the SC geometry. However in the case of long zigzag GNRs, which are always metallic, both the geometries yield comparable conductivities. As concerns the GMR coefficients and the Fano factors, they are always anticorrelated with the conductivities, and typically the SC GMR effect is higher than the EC one. Moreover,

practically in all the cases the range of the appearance of the so-called inverse (negative) GMR is strongly reduced in the SC geometry.

The new insight provided by this study is that high aspect ratio (wide and short) GNRs appear good candidates for interconnects in miniaturized electronic devices due to their preferential EC (edge) type conductance. As concerns miniaturization in spintronics, the short EC armchair GNRs, with $GMR \sim 20\%$ seem also quite attractive.

Acknowledgments

This work was supported by the Polish Ministry of Science and Higher Education as a research project No. N N202 199239 for 2010-2013.

References

- [1] Mann D, Javey A, Kong J, Wang Q and Dai H 2003 *Nano Letters* **3** 15141
- [2] Song X, Han X, Fu Q, Xu J and Wang N, Yu D 2009 *Nanotechnology* **20** 195202
- [3] Nemeč N and Tomanek D 2008 *Phys. Rev. B* **77** 125420
- [4] Matsuda Y, Deng W-Q and Goddard W A 2010 *J. Phys. Chem. C*, **114** 17845
- [5] Giovannetti G, Khomyakov P A, Brocks G, Karpan V M, van den Brink J and Kelly P J 2008 *Phys. Rev. Lett.* **101** 026803
- [6] Maassen J, Ji W and Guo H 2011 *Nano Lett.* **11** 151
- [7] Nagashio K, Nishimura T, Kita K and Toriumi A 2010 *Appl. Phys. Lett.* **97** 143514
- [8] Cottet A, Kontos T, Sahoo S, Man H T, Choi M-S, Belzig W, Bruder C, Morpurgo A F and Schönenberger C 2006 *Semicond. Sci. Technol.* **21** S78
- [9] Blanter Y M and Martin I 2007 *Phys. Rev. B* **76** 155433
- [10] Robinson J P and Schomerus H 2007 *Phys. Rev. B* **76** 115430
- [11] Krompiewski S 2005 *phys. status solidi (b)* **242** 226
- [12] Weymann I, Barnaś J and Krompiewski S 2008 *Phys. Rev. B* **78** 035422
- [13] Barraza-Lopéz S, Vanevic M, Kindermann M and Chou M Y 2010 *Phys. Rev. Lett.* **104** 076807
- [14] Krompiewski S 2009 *Phys. Rev. B* **80** 075433
- [15] Xia F, Perebeinos V, Lin Y-m, Wu Y and Avouris P 2011 *Nature Nanotech.* **6** 179
- [16] Stokbro K, Engelund M and Blom A *Preprint cond-mat/1202.0171v1*
- [17] Krompiewski S 2011 *Nanotechnology* **22** 445201
- [18] Liang W J, Bockrath M, Bozovic D, Hafner J H, Tinkham M and Park H 2001 *Nature* **411** 665
- [19] Javey A, Guo J, Wang Q, Lundstrom M, and Dai H 2003 *Nature* **424** 654
- [20] Miao F, Wijeratne S, Zhang Y, Coskun U C, Bao W and Lau C N 2007 *Science* **317** 1530
- [21] Du X, Skachko I, Barker A and Andrei E Y 2008 *Nature Nanotechnol.* **3** 491
- [22] Zhou Benhu, Chen Xiongwen, Wang Haiyan, Ding Kai-He and Zhou Guanghui 2010 *J. Phys.: Condens. Matter* **22** 445302
- [23] Zhou Benhu, Chen Xiongwen, Zhou Benliang, Ding Kai-He and Zhou Guanghui 2011 *J. Phys.: Condens. Matter* **23** 135304
- [24] Tworzydło J, Trauzettel B, Titov M, Rycerz A and Beenakker C W J 2006 *Phys. Rev. Lett.* **96** 246802
- [25] Danneau R, Wu F, Craciun M F, Russo S, Tomi M Y, Salmilehto J, Morpurgo A F, Hakonen P J 2008 *J. Low. Temp. Phys* **153** 374
- [26] Garca N, Esquinazi P, Barzola-Quiquia J, Ming B and Spoddig D 2008 *Phys. Rev. B* **78** 035413
- [27] Venugopa A, Colombo L, and Vogel E M 2010 *Appl. Phys. Lett.* **96** 013512
- [28] Yokoyama T and Linder J 2011 *Phys. Rev. B* **83** 081418